Electronic Supplementary Information for: UV-Vis Spectral Simulation of Polysulfur Species Using the Nuclear Ensemble Approximation

Robert Skog[†] and Benjamin N. Frandsen[*,†,‡]

†*Department of Chemistry, University of Helsinki, A. I. Virtasen aukio 1, FI-00560 Helsinki, Finland*

‡*Aerosol Physics Laboratory, Tampere University, Korkeakoulunkatu 3, FI-33720, Tampere, Finland*

E-mail: benjamin.frandsen@helsinki.fi

Table of Contents

List of Figures

List of Tables

A1 Benchmark calculations

For the benchmark calculations, we performed initial spectral simulation tests using EOM-CCSD, and with the B2PLYP, B3LYP, BHandHLYP, CAM-B3LYP, LC-ωHPBE, M05-2X, M06-2X, PBE0, ωB2PLYP, ωB97X-D3, and ωPBEPP86 density functionals. Basis sets used with these methods were aug-cc-pV(T+d)Z, jul-cc-pV(T+d)Z, jun-cc-pV(T+d)Z, may-cc-pV(T+d)Z, cc-pV(T+d)Z, def2-QZVPD, def2-TZVPPD, def2-TZVPD, aug-pc-2, aug-pcseg-2, pc-2, pcseg-2, and 6-311++G(3df,3pd). The best and most consistent spectral simulation levels of theory were EOM-CCSD, BHandHLYP, CAM-B3LYP, ωB97X-D3, and ωB2PLYP, combined with the aug-cc-pV(T+d)Z basis set. The simulated spectra of the benchmark molecules (CS_2, H_2S, HO_2, O_3, OCS, PH_3, SO_2, and SO_3) are shown in Figures A1-A8, and below we discuss the results in more detail.

For the experimental spectrum of CS_2 we use a composite of the results by Grosch *et al.*[1] (206-350 nm), Sunanda *et al.*[2] (185-206 nm), and Rabalais *et al.*[3] (180-185 nm). As seen in Figure A1, the levels of theory benchmarked in this work predict the first absorption peak to be around 315 nm, which is in good agreement with the experimental spectrum. The absorption cross section for this first peak is slightly underestimated in all simulated spectra. The second, stronger absorption region below 230 nm is qualitatively modeled quite well.

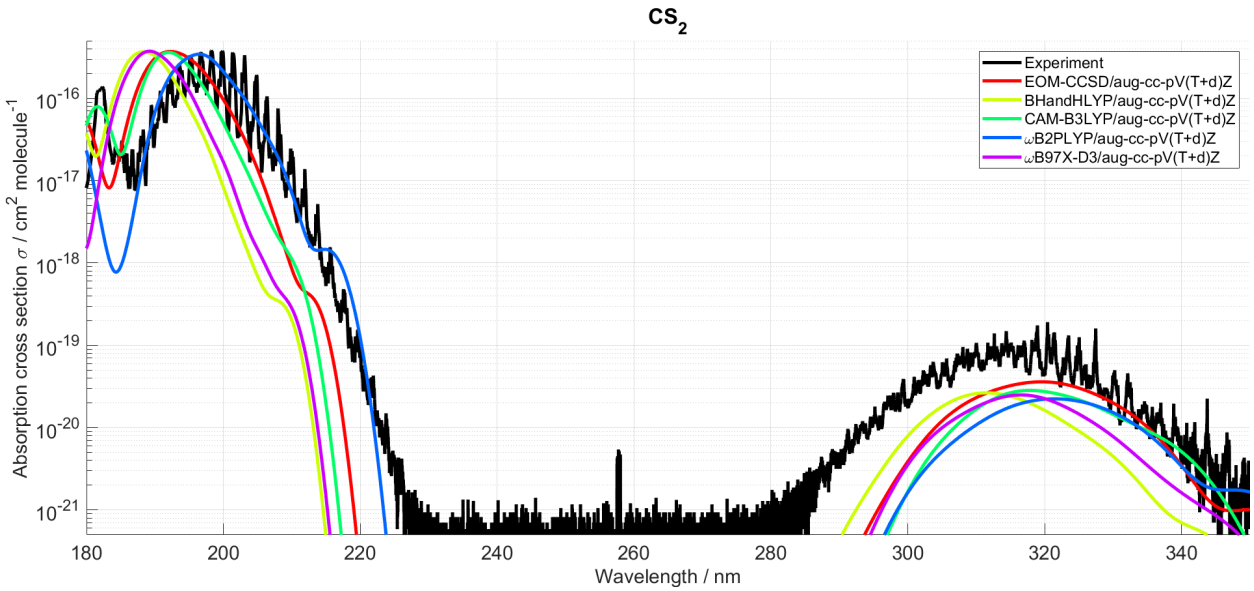

Figure A1: Simulated spectra for the CS_2 molecule, compared to the experimental results by Grosch *et al.*[1] (206-350 nm), Sunanda *et al.*[2] (185-206 nm), and Rabalais *et al.*[3] (180-185 nm). The ten lowest vertical excitations are included in the simulated spectra.

The experimental spectrum of H_2S used for comparison is taken from the work of Wu and Chen[4] (160-260 nm). The peak of the experimental spectrum is found around 195 nm, as seen in Figure A2. Most spectral simulation levels of theory correctly predict this peak position and the absorption cross section, the only exception being the CAM-B3LYP/aug-cc-pV(T+d)Z spectrum, which red-shifts the peak by approximately 10 nm. The absorption cross section decreases after 195 nm in the experimental spectrum. Although all methods reproduce the decrease, the magnitude of this decrease is overestimated.

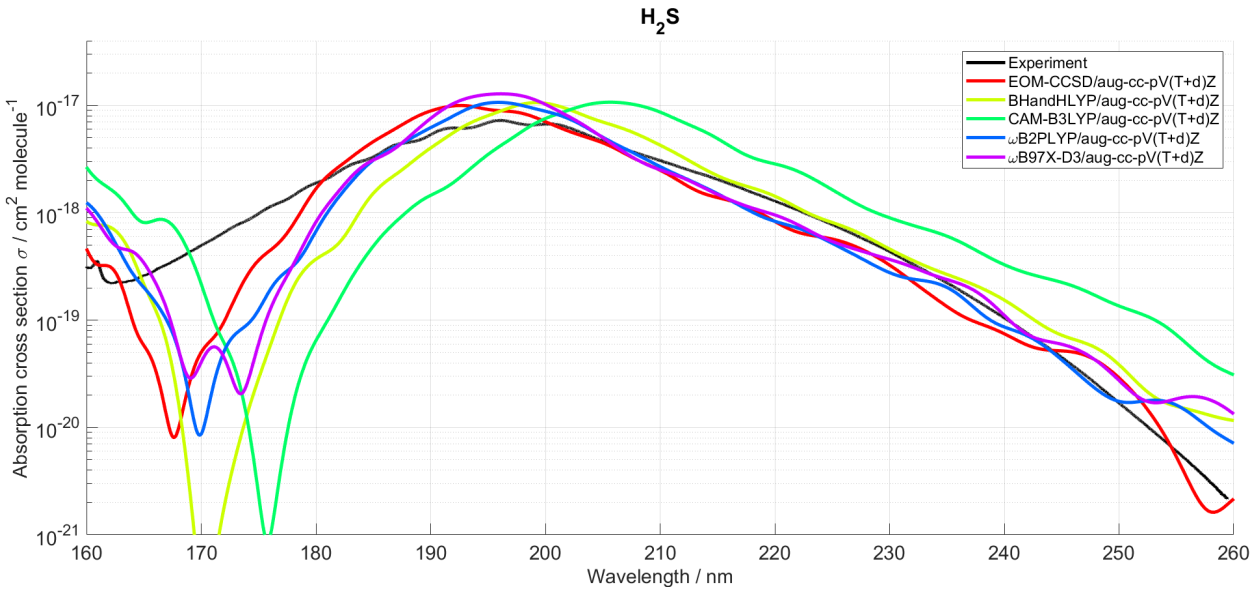

Figure A2: Simulated spectra for the H_2S molecule, compared to the results by Wu and Chen[4] (160-260 nm). The ten lowest vertical excitations are included in the simulated spectra.

The HO_2 radical is an interesting test, as the results will show if the nuclear ensemble approximation is able to qualitatively simulate the UV-Vis absorption spectra of other species than closed-shell molecules. In Figure A3, the simulated spectra using different levels of theory are compared with the JPL 2010 recommendation[5] (190-260 nm). The general shape of the experimental spectrum is recovered quite well by all simulated spectra, although the absorption cross section is slightly underestimated towards the longer wavelengths.

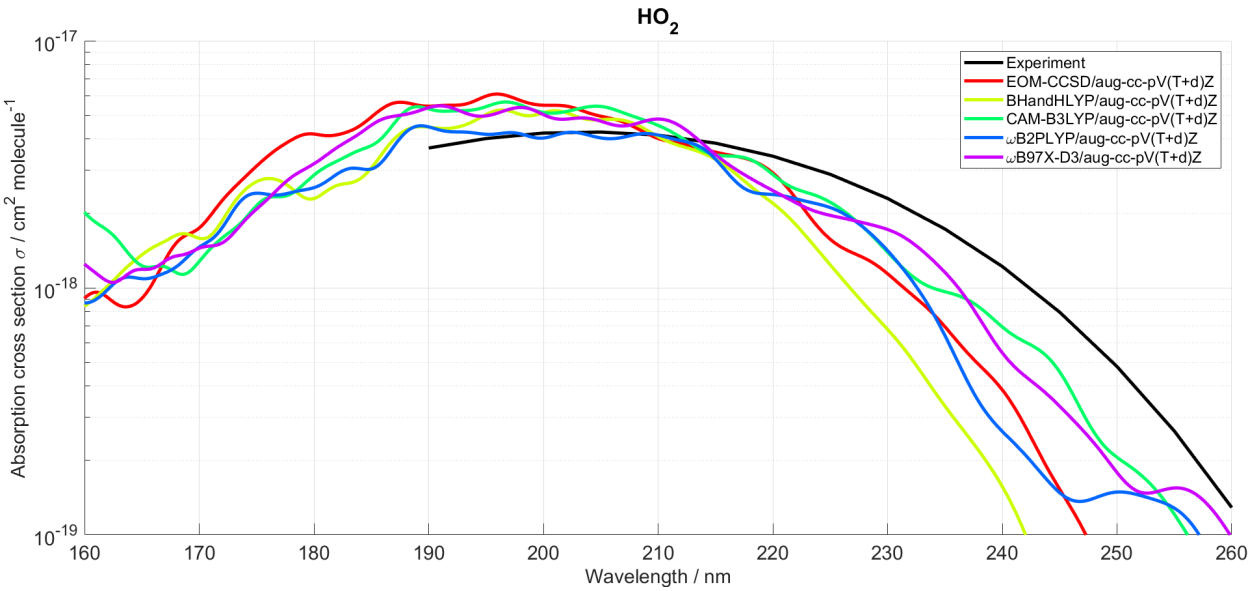

Figure A3: Simulated spectra for the HO_2 radical, compared to the JPL 2010 recommendation[5] (190-260 nm). The ten lowest vertical excitations are included in the simulated spectra.

Another interesting system is O_3 due to the more exotic electronic structure, as O_3 is a classic example of a multireference system.[12] The experimental spectrum used for comparison is the JPL 2010 recommendation[5] (120-350 nm). None of the simulated spectra in Figure A4 reproduce the absorption over 500 nm found in the experimental one (the Chappuis and Wulf bands). The peak around 250 nm found in the experimental spectrum is found in every simulated spectrum; however, it has been blue-shifted by 10-30 nm. In addition, all simulated spectra have a sharp drop in the absorption cross section below 200 nm, which is not found in the experimental spectrum. As noted in Section 3.1 of the Article, the spectral simulation methods are all single reference approaches. A more fair benchmark would be using a multireference method as the spectrum simulation level of theory.

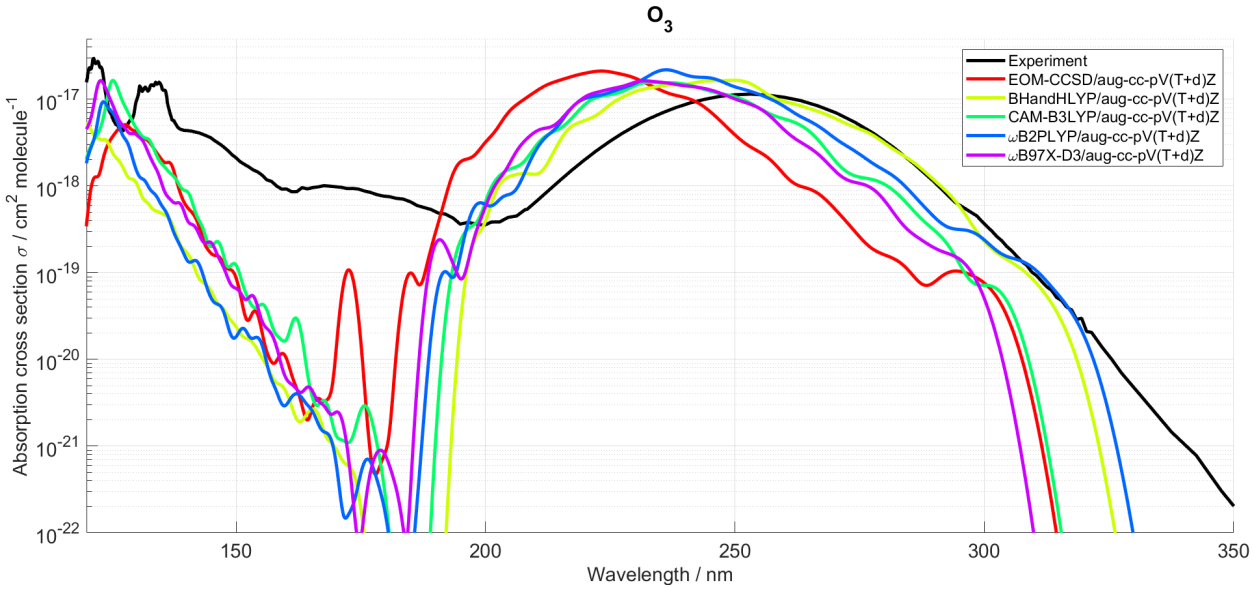

Figure A4: Simulated spectra for the O_3 molecule, compared to the JPL 2010 recommendation[5] (160-350 nm). The ten lowest vertical excitations are included in the simulated spectra.

Next, in Figure A5, we present the results for OCS. The experimental spectrum used for comparison is a composite of the JPL 2010 recommendation[5] (258-280 nm), and the results by Limão-Vieira *et al.*[6] (140-258 nm). Although the simulated spectra do not replicate the vibrational structure in the experimental spectrum, all levels of theory reproduce the average absorption extremely well. The only minor deviation can be seen around 200 nm. Here, the TD-DFT levels of theory predict a much smaller absorption cross section compared to the experimental spectrum.

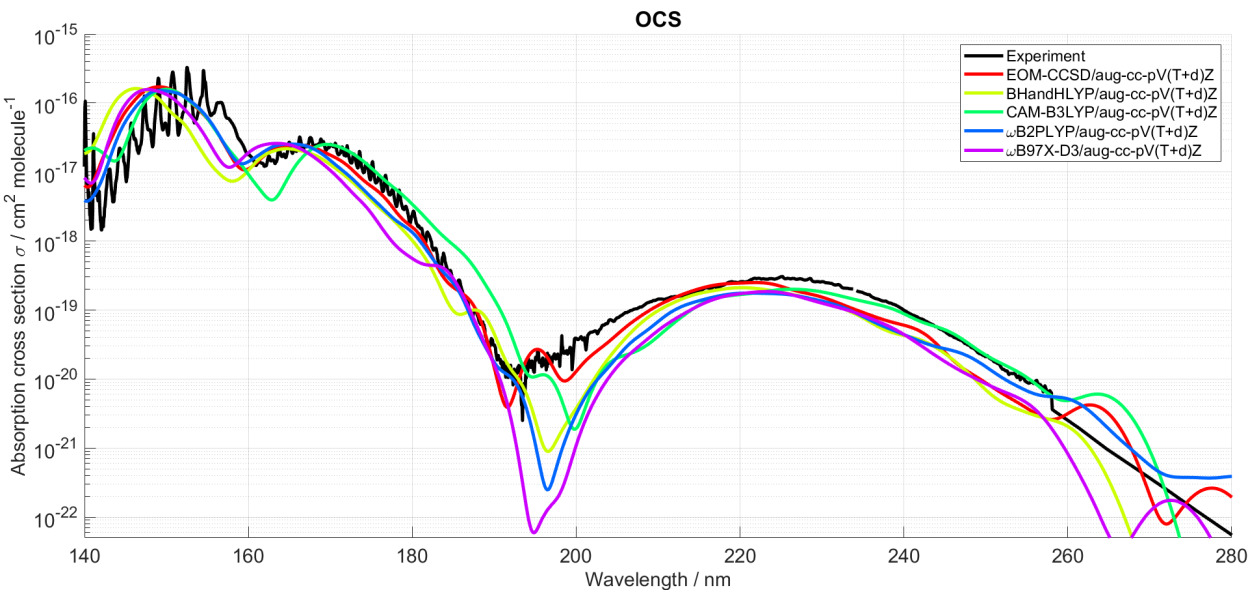

Figure A5: Simulated spectra for the OCS molecule, compared to the JPL 2010 recommendation[5] (258-280 nm) and the work by Limão-Vieira *et al.*[6] (140-258 nm). The ten lowest vertical excitations are included in the simulated spectra.

Similarly, good performance is also seen in the case of PH_3, in Figure A6. Here, the results by Chen *et al.*[7] are used as the experimental comparison. Although some minor deviations from the experimental spectrum can be found between 140-155 nm, and at wavelengths longer than 205 nm, the simulated spectra are overall in good agreement with the experimental one. The 205 nm region is the drop-off region, and not captured well due to limited sampling of geometries. For CAM-B3LYP/aug-cc-pV(T+d)Z spectrum, a sharp drop in the absorption cross section is seen starting at 140 nm. This is an artifact of only including the ten lowest excited states in the spectral simulations. For a more complete spectrum, more excited states should be included.

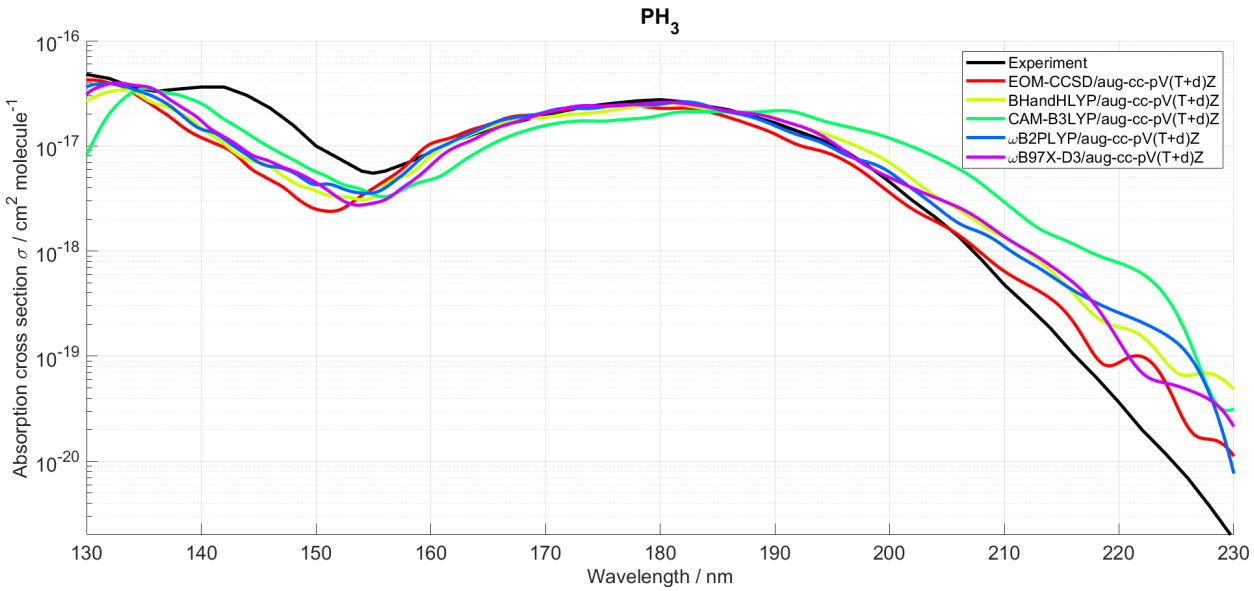

Figure A6: Simulated spectra for the PH_3 molecule, compared to the experimental results by Chen *et al.*[7] (130-230 nm). The ten lowest vertical excitations are included in the simulated spectra.

The results for SO_2 are presented in Figure A7. Here, we use the compilation by Manatt and Lane[8] as the experimental comparison. SO_2 was also extensively used by Farahani *et al.*[13] to benchmark settings for NEA spectral simulations, such as the broadening factor and the number of geometries in the ensemble. As seen in Figure A7, the experimental composite spectrum clearly shows vibrational structure, which the NEA cannot reproduce due to not calculating Franck-Condon factors. However, the wavelength range and absorption cross sections for the two first peaks (at 280 and 200 nm) are reproduced quite accurately.

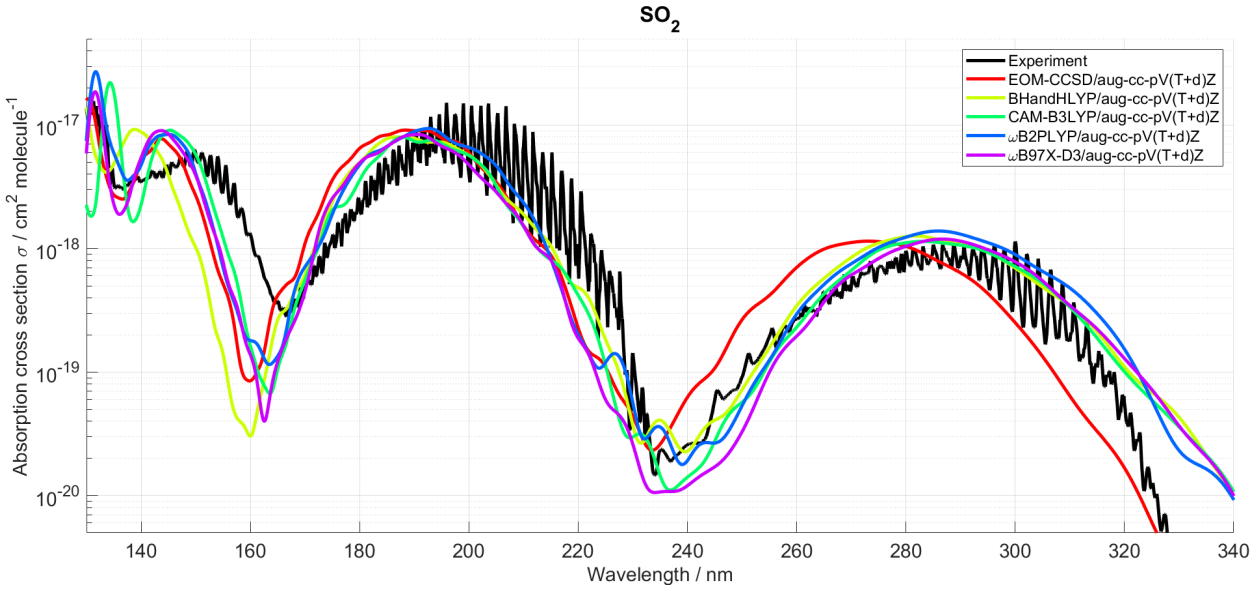

Figure A7: Simulated spectra for the SO_2 molecule, compared to the compilation by Manatt and Lane[8] (130-340 nm). The ten lowest vertical excitations are included in the simulated spectra.

The results by Burkholder and McKeen[9] (196-300 nm), and Hintze *et al.*[10] (140-194 nm) are used as the experimental comparison, and visualized with the simulated spectra in Figure A8. The experimental spectrum shows a steady increase in the absorption cross section towards shorter wavelengths, with a steeper increase observed below 160 nm. Although the BHandHLYP/aug-cc-pV(T+d)Z spectrum slightly underestimates the absorption cross section at wavelengths longer than 200 nm, overall, the simulated spectra are in good agreement with the experimental spectrum. The increase in the absorption cross section below 160 is also captured very well by all simulated spectra.

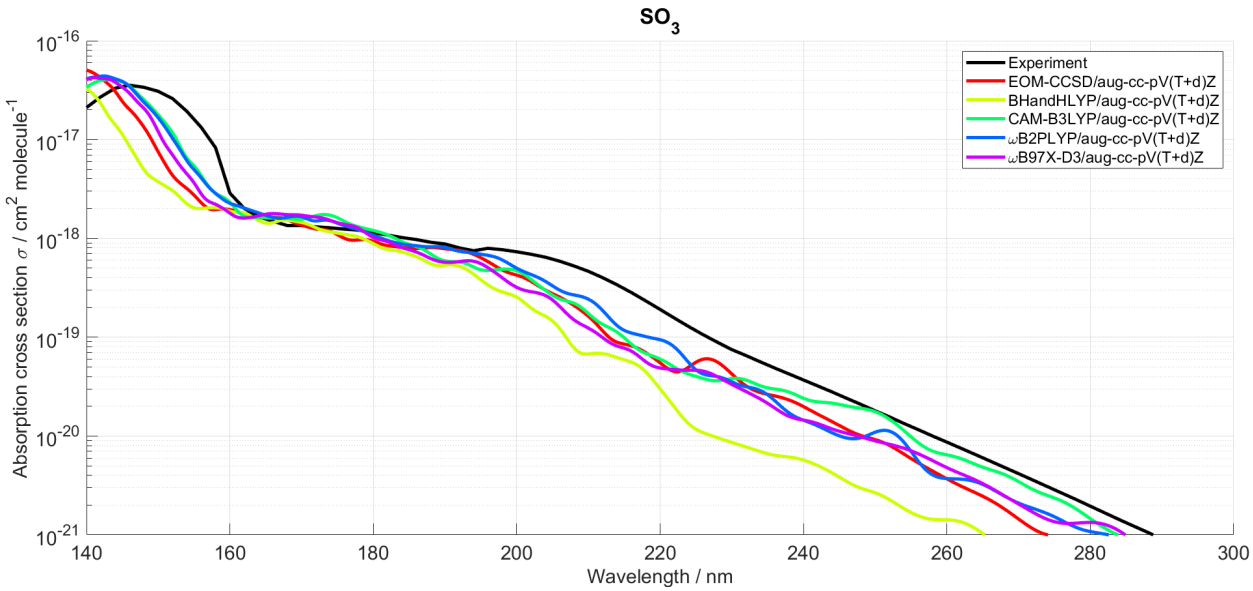

Figure A8: Simulated spectra for the SO_3 molecule, compared to the results by Burkholder and McKeen[9] (196-300 nm), Hintze *et al.*[10] (140-194 nm). The ten lowest vertical excitations are included in the simulated spectra.

What we did not benchmark in this work are the different methods that can be used to create the nuclear ensemble. One method, often used in early works, is Boltzmann sampling; running Born-Oppenheimer ground-state dynamics and taking snapshots from these as the ensemble. However, as noted by Barbatti and Sen,[14] this will not completely recover the zero-point energy, thereby leading to artificially narrow bands in the final spectrum. Another method - the one used in this work - is quantum sampling by creating a Wigner distribution based on normal mode displacements. This is an attractive approach, as only the ground state geometry and normal modes of the system are required. It also correctly recovers the zero-point energy.[14] But the Wigner approach also suffers from some problems. Other local minima, which might contribute to the UV-Vis spectrum, will not be included in the ensemble.[15] This shortcoming can be rectified by performing separate spectra simulations for the different minima. In addition, the combination of using the harmonic approximation for low-frequency normal modes and creating the ensemble through normal mode distortions can lead to unphysical geometries. These geometries cause unphysical features in the final spectrum.[15,16] More recently, quantum thermostat ground-state dynamics has been used

successfully to simulate the spectra of atmospherically relevant molecules.[16,17]

A2 Calculations and spectral simulations for the S_x species

A2.1 Configuration state function weights for the S_2, S_3 and S_4 structures

Tables A1, A2 and A3 show the weights of the five first configuration state functions (CSFs) from the CASSCF calculations when calculating energies using NEVPT2/aug-cc-pV(T+d)Z [NEVPT2(12,8)/aug-cc-pV(T+d)Z for S_2, NEVPT2(18,12)/aug-cc-pV(T+d)Z for S_3, and NEVPT2(24,16)/aug-cc-pV(T+d)Z for S_4] for the CCSD/aug-cc-pV(T+d)Z optimized S_2, S_3 and S_4 geometries. These weights are calculated as the sum of the squares of the CI coefficients for all configuration state functions that give arise to a particular configuration.

Miliordos and Xantheas[12] evaluated the biradical character (β) for several triatomic molecules consisting of oxygen and sulfur. The definition for β used was

$$\beta = \frac{2 \times c_2^2}{(c_1^2 + c_2^2)}, \tag{1}$$

where c_1 and c_2 are CI coefficients for the two leading configurations. There are two extreme cases; $\beta = 0$ indicates no biradical character, while $\beta = 1$ indicates perfect biradical character. For S_3, the reported value was $\beta = 0.108$.[12] We also report the β values for all S_2-S_4 structures in Tables A1, A2 and A3.

Table A1: The weights for the five first configuration state functions (CSFs) and the calculated β values for the S_2 species studied in this work

Structure	CSF weights					β
$^3S_2$	0.94828	0.02093	0.01030	0.01030	0.00501	0.043
$^1S_2$	0.46534	0.46534	0.02168	0.02168	0.00841	1.000

Table A2: The weights for the five first configuration state functions (CSFs) and the calculated β values for the S_3 species studied in this work

Structure	CSF weights					β
linear-S_3	0.88362	0.04558	0.01223	0.00670	0.00576	0.098
cyclic-S_3	0.92766	0.00782	0.00782	0.00706	0.00706	0.017
linear-$^3S_3$	0.87933	0.05616	0.00695	0.00567	0.00506	0.120

Table A3: The weights for the five first configuration state functions (CSFs) and the calculated β values for the S_4 species studied in this work

Structure	CSF weights					β
cis-S_4	0.81196	0.08246	0.01231	0.00699	0.00542	0.184
trans-S_4	0.79343	0.10478	0.01005	0.00447	0.00406	0.233
cis-$^3S_4$	0.90271	0.01610	0.00484	0.00395	0.00313	0.035
trans-$^3S_4$	0.90730	0.01103	0.00517	0.00394	0.00384	0.024
cyclic-S_3(S)	0.88746	0.00878	0.00824	0.00680	0.00566	0.020
cyclic-S_4	0.91189	0.00705	0.00705	0.00510	0.00510	0.015
trigonal-S_4	0.88412	0.01169	0.01169	0.00833	0.00833	0.026
trigonal-$^3S_4$	0.86989	0.01089	0.00932	0.00532	0.00400	0.025

A2.2 Simulated spectra for S_2

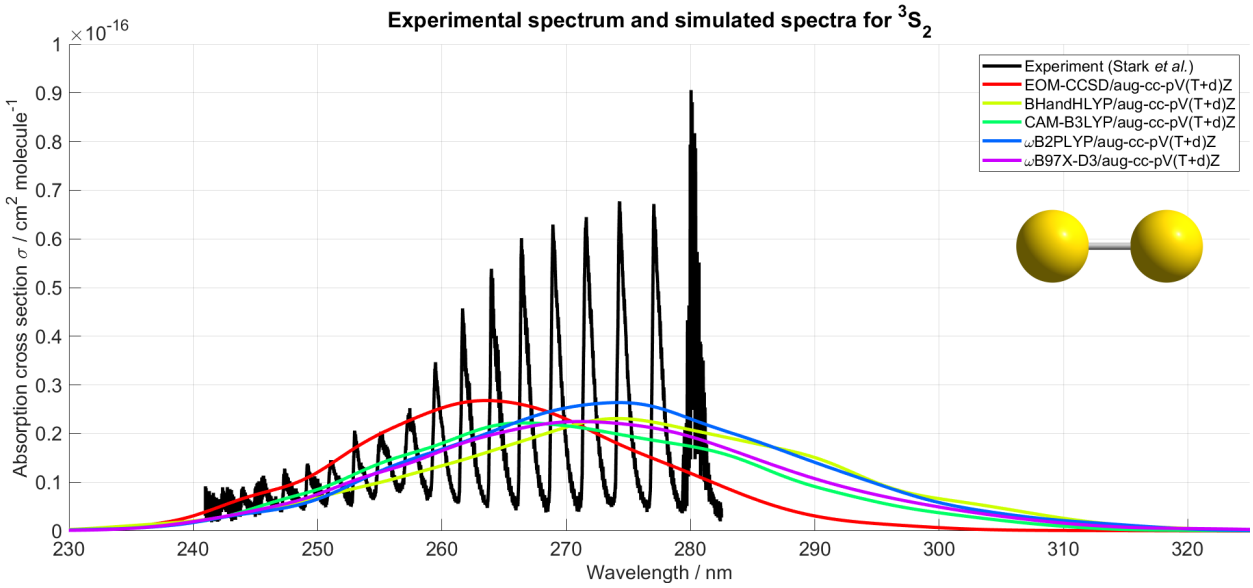

Figure A9: The simulated spectra for S_2, compared to the experimental spectrum by Stark *et al.*[11]

A2.3 Additional vertical excitation calculations and spectral scaling for the S_3 and S_4 systems

Note that in all of these additional single-point vertical excitation calculations, geometries optimized at the CCSD/aug-cc-pV(T+d)Z level of theory were used (meaning that the geometry was the same in all vertical excitation calculations).

Table A4: Three lowest vertical excitation energies (in nm) and oscillator strengths (in parenthesis, dimensionless) calculated at different levels of theory for the CCSD/aug-cc-pV(T+d)Z optimized linear-S_3 structure. All calculations use the aug-cc-pV(T+d)Z basis set, which has been omitted for brevity

VEE calculation method	$S_1 \leftarrow S_0$	$S_2 \leftarrow S_0$	$S_3 \leftarrow S_0$
BHandHLYP	721 (0.000)	720 (0.000)	383 (0.119)
CAM-B3LYP	739 (0.000)	731 (0.000)	385 (0.108)
ωB97X-D3	732 (0.000)	731 (0.000)	385 (0.113)
ωB2PLYP	721 (0.000)	722 (0.000)	386 (0.141)
EOM-CCSD	675 (0.000)	656 (0.000)	362 (0.133)
EOM-CC3	710 (0.000)	685 (0.000)	372 (0.099)
MC-RPA[a]	657 (0.000)	656 (0.000)	372 (0.108)

[a] Calculated using MC-RPA(18,12) on top of a CASSCF(18,12) reference.

Table A5: Three lowest vertical excitation energies (in nm) and oscillator strengths (in parenthesis, dimensionless) calculated at different levels of theory for the CCSD/aug-cc-pV(T+d)Z optimized *cis*-S_4 structure. All calculations use the aug-cc-pV(T+d)Z basis set, which has been omitted for brevity

VEE calculation method	$S_1 \leftarrow S_0$	$S_2 \leftarrow S_0$	$S_3 \leftarrow S_0$
BHandHLYP	679 (0.000)	666 (0.000)	539 (0.089)
CAM-B3LYP	682 (0.000)	662(0.000)	537 (0.083)
ωB97X-D3	692 (0.000)	657 (0.000)	543 (0.087)
ωB2PLYP	681 (0.000)	654 (0.000)	534 (0.112)
EOM-CCSD	601 (0.000)	596 (0.000)	454 (0.110)
EOM-CC3	613 (0.000)	606 (0.000)	465 (0.075)
MC-RPA[a]	615 (0.000)	603 (0.000)	470 (0.081)

[a] Calculated using MC-RPA(24,18) on top of a CASSCF(24,18) reference.

Table A6: Three lowest vertical excitation energies (in nm) and oscillator strengths (in parenthesis, dimensionless) calculated at different levels of theory for the CCSD/aug-cc-pV(T+d)Z optimized *trans*-S_4 structure. All calculations use the aug-cc-pV(T+d)Z basis set, which has been omitted for brevity

VEE calculation method	$S_1 \leftarrow S_0$	$S_2 \leftarrow S_0$	$S_3 \leftarrow S_0$
BHandHLYP	949 (0.000)	648 (0.124)	503 (0.000)
CAM-B3LYP	958 (0.000)	654 (0.115)	505 (0.000)
ωB97X-D3	965 (0.000)	660 (0.123)	490 (0.000)
ωB2PLYP	966 (0.000)	664 (0.153)	495 (0.000)
EOM-CCSD	819 (0.000)	553 (0.176)	488 (0.000)
EOM-CC3	826 (0.000)	557 (0.108)	545 (0.000)
MC-RPA[a]	798 (0.000)	555 (0.124)	540 (0.000)

[a] Calculated using MC-RPA(24,18) on top of a CASSCF(24,18) reference.

The results from the additional vertical excitation calculations using MC-RPA(18,12)/aug-cc-pV(T+d)Z and MC-RPA(24,18)/aug-cc-pV(T+d)Z were used to scale the EOM-CCSD/aug-cc-pV(T+d)Z spectra for the linear-S_3, *cis*-S_4, and *trans*-S_4 structures. The MR-RPA results were chosen specifically due to the non-negligible amount of multiconfigurational character present in these structures. The transition wavelength in the spectra were shifted based on the difference in excitation energy between the MC-RPA/aug-cc-pV(T+d)Z and the EOM-CCSD/aug-cc-pV(T+d)Z calculations. Similarly, the absorption cross sections in the spectra were scaled based on the oscillator strength ratio between the MC-RPA/aug-cc-pV(T+d)Z and the EOM-CCSD/aug-cc-pV(T+d)Z calculations. The transitions with the largest oscillator strength were used to derive the energy difference and the oscillator strength ratio.

A2.4 Spectra for *cis*-$^3S_4$ and *trans*-$^3S_4$

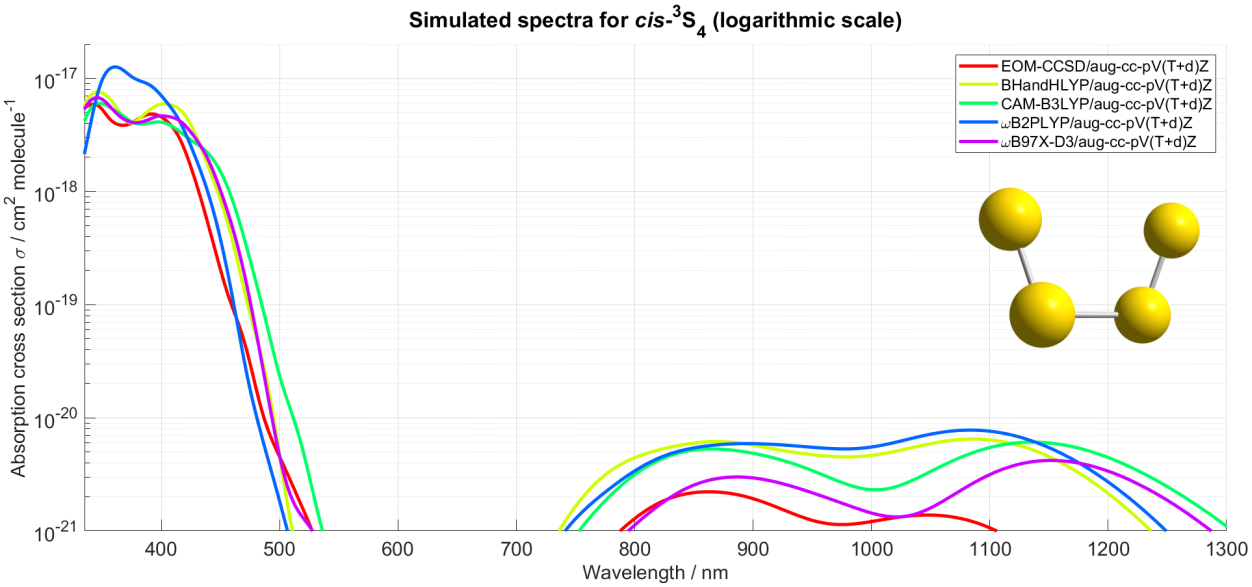

Figure A10: The simulated spectra for *cis*-$^3S_4$, using a logarithmic scale for the y axis.

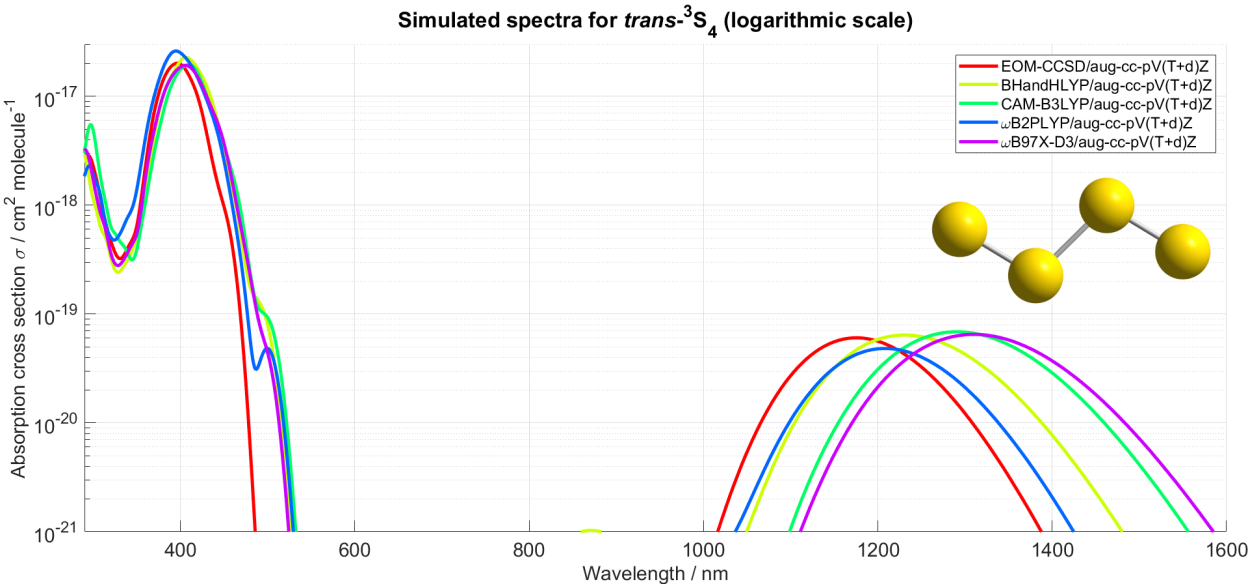

Figure A11: The simulated spectra for *trans*-$^3S_4$, using a logarithmic scale for the y axis.

A3 Geometries for benchmark calculation molecules

All geometries have been optimized at the CCSD/aug-cc-pV(T+d)Z level of theory. The second line for each geometry indicates the charge and the multiplicity, respectively.

CS_2

0 1

C	0.000000000000	0.000000000000	0.000000000000
S	0.000000000000	0.000000000000	-1.553470607772
S	0.000000000000	0.000000000000	1.553470607772

H_2S

0 1

S	0.000000000000	0.000000000000	0.054820238821
H	0.000000000000	-0.965615121466	-0.869554014673
H	0.000000000000	0.965615121466	-0.869554014673

HO_2

0 2

O	-0.633014726595	-0.066177276894	0.000000000000
O	0.691719502140	0.012175225477	0.000000000000
H	-0.931687430157	0.857051752364	0.000000000000

O_3

0 1

O	0.000000000000	0.000000000000	0.431082820961
O	0.000000000000	-1.069193196374	-0.215541413126
O	0.000000000000	1.069193196374	-0.215541413126

OCS

0 1

C	0.000000000000	0.000000000000	0.528016265866
S	0.000000000000	0.000000000000	-1.039122064187
O	0.000000000000	0.000000000000	1.680952317531

PH_3

0 1

P	0.000000206379	0.000000518594	-0.067716965726
H	-0.949109670312	0.721097136958	0.693723258252
H	1.099046381620	0.461392543294	0.693726401565
H	-0.149943024392	-1.182505560862	0.693714262239

SO_2
0 1

S	0.000000000000	0.000000000000	0.361737814970
O	0.000000000000	-1.233788329150	-0.361537002787
O	0.000000000000	1.233788329150	-0.361537002787

SO_3
0 1

S	-0.000004677927	0.000000396883	0.000000000000
O	-0.708919657187	-0.000000264589	1.227903767014
O	1.417848670227	-0.000000264589	0.000000000000
O	-0.708919657187	-0.000000264589	-1.227903767014

A4 Geometries for all S_x species

A4.1 Geometries optimized using ωB97X-D/aug-cc-pV(T+d)Z

The second line for each geometry indicates the charge and the multiplicity, respectively.

A4.1.1 S_2

$^3S_2$
0 3

S	0.000000000000	0.000000000000	0.941527000000
S	0.000000000000	0.000000000000	-0.941527000000

$^1S_2$

0 1

S	0.000000000000	0.000000000000	0.941486000000
S	0.000000000000	0.000000000000	-0.941486000000

A4.1.2 S_3

linear-S_3

0 1

S	0.000000000000	0.000000000000	0.654263000000
S	0.000000000000	1.623641000000	-0.327132000000
S	0.000000000000	-1.623641000000	-0.327132000000

cyclic-S_3

0 1

S	0.000000000000	0.000000000000	1.197254000000
S	0.000000000000	1.036789000000	-0.598627000000
S	0.000000000000	-1.036789000000	-0.598627000000

linear-$^3S_3$

0 3

S	0.000000000000	0.000000000000	0.916042000000
S	0.000000000000	1.416778000000	-0.458021000000
S	0.000000000000	-1.416778000000	-0.458021000000

A4.1.3 S_4

Minima.

***cis*-S_4**

0 1

S	1.615276000000	0.900980000000	0.000000000000
S	1.022856000000	-0.900982000000	0.000001000000
S	-1.022859000000	-0.900981000000	-0.000001000000
S	-1.615272000000	0.900983000000	0.000000000000

***trans*-S_4**

0 1

S	0.938185000000	2.265332000000	0.000000000000
S	0.938185000000	0.352975000000	0.000000000000
S	-0.938185000000	-0.352975000000	0.000000000000
S	-0.938185000000	-2.265332000000	0.000000000000

***cis*-^{3}S$_4$**

0 3

S	-0.632921000000	1.577488000000	0.898365000000
S	-0.632921000000	0.929320000000	-0.898365000000
S	0.632921000000	-0.929320000000	-0.898365000000
S	0.632921000000	-1.577488000000	0.898365000000

***trans*-^{3}S$_4$**

0 1

S	1.047993000000	2.194710000000	0.000000000000
S	1.047993000000	0.266055000000	0.000000000000
S	-1.047993000000	-0.266055000000	0.000000000000
S	-1.047993000000	-2.194710000000	0.000000000000

cyclic-S$_3$(S)

0 1

S	1.222210000000	1.043924000000	-0.168225000000
S	-0.427845000000	0.000002000000	0.685864000000
S	1.222290000000	-1.043899000000	-0.168218000000
S	-2.016655000000	-0.000027000000	-0.349421000000

cyclic-S_4

0 1

S	0.993153000000	1.016325000000	0.308764000000
S	1.016325000000	-0.993154000000	-0.308764000000
S	-0.993153000000	-1.016324000000	0.308765000000
S	-1.016325000000	0.993152000000	-0.308765000000

trigonal-S_4

0 1

S	0.000000000000	0.000000000000	0.000000000000
S	0.000000000000	1.891259000000	0.000000000000
S	-1.637879000000	-0.945630000000	0.000000000000
S	1.637879000000	-0.945630000000	0.000000000000

trigonal-$^3S_4$

0 3

S	-0.310397000000	0.317996000000	0.000000000000
S	0.931190000000	1.773495000000	0.000000000000
S	-0.310397000000	-1.045746000000	1.436747000000
S	-0.310397000000	-1.045746000000	-1.436747000000

Transition states.

S_4, TS1 (*cis*-S_4 → *cis*-S_4)

0 1

S	-1.232530000000	0.936706000000	0.000000000000
S	-1.232529000000	-0.936706000000	0.000000000000
S	1.232529000000	-0.936706000000	0.000000000000
S	1.232530000000	0.936706000000	0.000000000000

S_4, TS2 (*cis*-S_4 → cyclic-S_3(S))

0 1

S	-1.677237000000	0.937203000000	0.150297000000
S	-1.056171000000	-0.883254000000	-0.406898000000
S	0.748886000000	-0.603823000000	0.555909000000
S	1.984522000000	0.549875000000	-0.299308000000

S_4, TS3 (*trans*-S_4 → cyclic-S_3(S))

0 1

S	-1.966116000000	-0.655828000000	-0.203718000000
S	-0.862745000000	1.011366000000	-0.039531000000
S	0.599186000000	-0.230515000000	0.599208000000
S	2.229675000000	-0.125023000000	-0.355960000000

S_4, TS4 (*trans*-S_4 → cyclic-S_4)

0 1

S	1.391488000000	0.848196000000	0.355174000000
S	0.984692000000	-0.848197000000	-0.501903000000
S	-0.984694000000	-0.848197000000	0.501902000000
S	-1.391486000000	0.848199000000	-0.355174000000

S_4, TS5 (cyclic-S_3(S) → cyclic-S_4)

0 1

S	1.855640000000	0.055943000000	-0.325344000000
S	-0.340217000000	1.153928000000	0.269572000000
S	0.187724000000	-0.937035000000	0.418021000000
S	-1.703147000000	-0.272836000000	-0.362248000000

S_4, TS6 (cyclic-S_3(S) → trigonal-S_4)

0 1

S	-1.186872000000	-1.364048000000	-0.122915000000
S	0.191513000000	0.013787000000	0.435721000000
S	-1.002791000000	1.439420000000	-0.131860000000
S	1.998149000000	-0.089159000000	-0.180947000000

A4.1.4 S_5

cyclic-S_5 (A)

0 1

S	-1.479976000000	-0.561263000000	-0.447733000000
S	0.000833000000	-1.557982000000	0.587116000000
S	1.480597000000	-0.559737000000	-0.447615000000
S	1.075961000000	1.340110000000	0.154041000000
S	-1.077413000000	1.338872000000	0.154191000000

$^3S_5$ (B)

0 3

S	1.646019000000	-0.576695000000	-0.442191000000
S	-0.000013000000	-1.290524000000	0.633078000000
S	-1.646086000000	-0.576697000000	-0.442132000000
S	-2.078500000000	1.221996000000	0.125585000000
S	2.078580000000	1.221920000000	0.125660000000

$^3S_5$ (C)

0 3

S	1.389535000000	0.046288000000	-0.876287000000
S	0.000000000000	1.341349000000	-0.000030000000
S	-1.389531000000	0.046322000000	0.876285000000
S	-2.537938000000	-0.716988000000	-0.479777000000
S	2.537934000000	-0.716970000000	0.479810000000

S_5 (D)

0	**1**		
S	-0.991325000000	-0.535885000000	-0.000078000000
S	-0.043745000000	1.252885000000	-0.000063000000
S	1.917950000000	0.709066000000	0.000070000000
S	2.003250000000	-1.217372000000	-0.000002000000
S	-2.886130000000	-0.208694000000	0.000073000000

S_5 (E)

0	**1**		
S	-0.972255000000	-0.202654000000	0.659122000000
S	-0.000013000000	1.547999000000	-0.000032000000
S	0.972233000000	-0.202712000000	-0.659067000000
S	2.600522000000	-0.571299000000	0.246403000000
S	-2.600487000000	-0.571334000000	-0.246425000000

S_5 (F)

0	**1**		
S	-2.016077000000	-0.000059000000	0.177986000000
S	-0.604688000000	-1.450262000000	-0.302516000000
S	2.468525000000	0.000018000000	-0.193014000000
S	0.757042000000	0.000020000000	0.620055000000
S	-0.604802000000	1.450283000000	-0.302511000000

S_5 (G)

0 1

S	1.645708000000	0.000042000000	0.809600000000
S	0.733875000000	1.432581000000	-0.369406000000
S	-2.214125000000	0.000011000000	0.649477000000
S	-0.899374000000	-0.000033000000	-0.720315000000
S	0.733917000000	-1.432601000000	-0.369356000000

S_5 (H)

0 1

S	-0.708406000000	0.068876000000	0.000001000000
S	0.962844000000	-1.142775000000	-0.000001000000
S	-2.385506000000	-0.820478000000	0.000000000000
S	-0.378152000000	1.926166000000	-0.000001000000
S	2.509219000000	-0.031789000000	0.000001000000

S_5 (I)

0 1

S	0.351047000000	0.000001000000	0.000003000000
S	1.283785000000	1.655288000000	-0.000006000000
S	1.283787000000	-1.655288000000	-0.000008000000
S	-1.459325000000	0.000001000000	-1.066018000000
S	-1.459294000000	-0.000003000000	1.066029000000

$^3S_5$ (J)

0 3

S	0.000003000000	0.000005000000	0.000001000000
S	-1.355354000000	1.352581000000	0.428726000000
S	-1.355352000000	-1.352583000000	-0.428731000000
S	1.355348000000	-0.428732000000	1.352576000000
S	1.355355000000	0.428730000000	-1.352573000000

A4.1.5 S_6

chair-S_6 (A)

0 1

S	-1.719438000000	-0.707043000000	0.444445000000
S	-1.471963000000	1.135481000000	-0.444428000000
S	-0.247397000000	-1.842479000000	-0.444426000000
S	1.471963000000	-1.135481000000	0.444428000000
S	1.719438000000	0.707043000000	-0.444445000000
S	0.247397000000	1.842479000000	0.444426000000

boat-S_6 (B)

0 1

S	-1.473457000000	0.400059000000	0.758417000000
S	-0.623040000000	1.851343000000	-0.375222000000
S	-1.473457000000	-1.276141000000	-0.383195000000
S	0.623040000000	-1.851343000000	-0.375222000000
S	1.473457000000	-0.400059000000	0.758417000000
S	1.473457000000	1.276141000000	-0.383195000000

S_6 (C)

0 1

S	-0.318533000000	1.482592000000	-0.949328000000
S	1.348417000000	0.000037000000	-0.676377000000
S	-1.291200000000	1.103726000000	0.713333000000
S	-1.291110000000	-1.103731000000	0.713292000000
S	1.871133000000	-0.000104000000	1.148525000000
S	-0.318708000000	-1.482520000000	-0.949445000000

S_6 (D)

0 1

S	1.232532000000	-0.042811000000	-0.706939000000
S	-0.136763000000	-1.641264000000	-0.023432000000
S	-0.198106000000	1.583929000000	-0.602258000000
S	-1.498338000000	0.931979000000	0.831744000000
S	-1.975789000000	-0.808764000000	-0.154765000000
S	2.576464000000	-0.023070000000	0.655650000000

$^3S_6$ (E)

0 3

S	1.872181000000	-1.093338000000	-0.976351000000
S	2.026853000000	-0.218434000000	0.709455000000
S	0.449552000000	1.311776000000	0.867398000000
S	-0.449551000000	1.311761000000	-0.867419000000
S	-2.026851000000	-0.218445000000	-0.709453000000
S	-1.872184000000	-1.093319000000	0.976370000000

S_6 (F)

0 1

S	-0.055580000000	1.504526000000	-0.479576000000
S	1.053855000000	-0.000001000000	0.658041000000
S	-1.890954000000	1.098432000000	0.169303000000
S	-1.890954000000	-1.098424000000	0.169322000000
S	2.839229000000	-0.000002000000	-0.037501000000
S	-0.055597000000	-1.504531000000	-0.479588000000

$^3S_6$ (G)

0 3

S	-0.912049000000	-1.531103000000	0.447634000000
S	-2.017507000000	-0.067649000000	-0.584067000000
S	0.912035000000	-1.531106000000	-0.447638000000
S	2.017501000000	-0.067662000000	0.584070000000
S	-1.931736000000	1.598766000000	0.398602000000
S	1.931755000000	1.598753000000	-0.398601000000

S_6 (H)

0 1

S	0.125834000000	1.015186000000	1.705512000000
S	-0.718265000000	0.931925000000	-0.295746000000
S	-0.125834000000	-1.015186000000	1.705512000000
S	0.718265000000	-0.931925000000	-0.295746000000
S	-0.125834000000	2.345157000000	-1.409767000000
S	0.125834000000	-2.345157000000	-1.409767000000

S_6 (I)

0 1

S	1.566334000000	-0.000005000000	-0.523929000000
S	0.000030000000	1.474537000000	-0.650499000000
S	-0.000031000000	-1.474515000000	-0.650547000000
S	-1.566334000000	0.000022000000	-0.523929000000
S	-2.421475000000	-0.000009000000	1.174453000000
S	2.421476000000	-0.000029000000	1.174451000000

S_6 (J)

0 1

S	-1.519691000000	-0.000003000000	-0.678769000000
S	0.046976000000	-1.477473000000	-0.452711000000
S	0.046917000000	1.477490000000	-0.452698000000
S	1.165335000000	0.000003000000	0.654717000000
S	2.995772000000	0.000006000000	0.137912000000
S	-2.735309000000	-0.000022000000	0.791549000000

A4.1.6 S_7

chair-S_7 (A)

0 1

S	1.959126000000	1.082511000000	-0.353543000000
S	0.422735000000	1.732333000000	0.740623000000
S	-1.255204000000	1.640733000000	-0.493778000000
S	1.959217000000	-1.082490000000	-0.353412000000
S	0.422724000000	-1.732303000000	0.740613000000
S	-1.255159000000	-1.640748000000	-0.493864000000
S	-2.253438000000	-0.000036000000	0.213361000000

boat-S_7 (B)

0 1

S	-1.108831000000	1.715275000000	-0.577028000000
S	-1.656224000000	0.535789000000	0.896103000000
S	-1.657734000000	-1.474111000000	0.176582000000
S	1.108923000000	1.715175000000	-0.577079000000
S	1.656286000000	0.535715000000	0.896080000000
S	1.657619000000	-1.474228000000	0.176627000000
S	-0.000040000000	-1.553616000000	-0.991285000000

S_7 (C)

0 1

S	-0.398477000000	-1.647630000000	-0.407025000000
S	1.465060000000	-1.594644000000	0.429296000000
S	-1.363117000000	0.000001000000	0.589143000000
S	-0.398471000000	1.647637000000	-0.407024000000
S	1.465067000000	1.594639000000	0.429297000000
S	2.376230000000	-0.000003000000	-0.502119000000
S	-3.146291000000	0.000001000000	-0.131568000000

$^3S_7$ (D)

0 3

S	2.229471000000	-0.919682000000	-0.484801000000
S	2.002785000000	0.825204000000	0.660165000000
S	0.652432000000	1.963385000000	-0.379068000000
S	1.007140000000	-2.280706000000	0.149652000000
S	-2.747166000000	-1.244755000000	0.427723000000
S	-1.948503000000	0.032338000000	-0.775352000000
S	-1.196160000000	1.624217000000	0.401682000000

$^3S_7$ (E)

0 3

S	2.866802000000	0.119242000000	0.336738000000
S	1.028341000000	0.455696000000	1.291663000000
S	0.000005000000	1.664641000000	-0.000007000000
S	2.714325000000	-1.407260000000	-0.845004000000
S	-2.714335000000	-1.407266000000	0.844995000000
S	-2.866797000000	0.119257000000	-0.336723000000
S	-1.028340000000	0.455690000000	-1.291662000000

S_7 (F)

0 1

S	-0.000102000000	1.961817000000	0.000071000000
S	0.353029000000	0.698831000000	-1.595041000000
S	1.107831000000	-1.008937000000	-0.729965000000
S	-0.353001000000	0.698709000000	1.595079000000
S	-1.107797000000	-1.009030000000	0.729906000000
S	-2.485429000000	-0.670714000000	-0.551923000000
S	2.485469000000	-0.670676000000	0.551874000000

S_7 (G)

0 1

S	0.982614000000	1.793772000000	-0.545478000000
S	1.461636000000	0.818227000000	1.201657000000
S	0.850200000000	-1.131443000000	0.647379000000
S	-1.033572000000	1.652603000000	-0.390970000000
S	-1.253377000000	-0.459942000000	-0.518058000000
S	-2.848090000000	-0.864916000000	0.447475000000
S	1.840588000000	-1.808301000000	-0.842006000000

A4.1.7 S_8

crown-S_8 (A)

0 1

S	-1.467023000000	1.829242000000	0.495390000000
S	-2.331019000000	0.256094000000	-0.494939000000
S	-1.829255000000	-1.467102000000	0.495115000000
S	-0.256083000000	-2.330933000000	-0.495320000000
S	0.256015000000	2.331023000000	-0.494934000000
S	1.829323000000	1.467014000000	0.495130000000
S	2.330953000000	-0.256006000000	-0.495302000000
S	1.467089000000	-1.829333000000	0.494859000000

twisted-S_8 (B)

0 1

S	0.000008000000	-1.661633000000	-1.013882000000
S	1.692417000000	-1.830023000000	0.097684000000
S	2.058653000000	0.059783000000	0.938779000000
S	1.702913000000	1.407792000000	-0.555833000000
S	-1.692401000000	-1.830037000000	0.097684000000
S	-2.058657000000	0.059766000000	0.938778000000
S	-1.702925000000	1.407780000000	-0.555833000000
S	-0.000010000000	2.386572000000	0.052623000000

***exo-endo*-S_8 (C)**

0 1

S	-0.843430000000	2.275662000000	0.386631000000
S	0.648608000000	1.795846000000	-0.875984000000
S	2.198369000000	0.996017000000	0.234358000000
S	2.198187000000	-0.996418000000	-0.234456000000
S	-2.002957000000	0.547649000000	0.839855000000
S	-2.003221000000	-0.547283000000	-0.839655000000
S	-0.843857000000	-2.275490000000	-0.386661000000
S	0.648301000000	-1.795983000000	0.875912000000

boat-S_8 (D)

0 1

S	-0.117521000000	-1.789647000000	1.074429000000
S	1.907008000000	-1.127297000000	0.615581000000
S	1.789662000000	-0.117520000000	-1.074429000000
S	1.127298000000	1.907004000000	-0.615580000000
S	-1.127298000000	-1.907006000000	-0.615579000000
S	-1.789661000000	0.117519000000	-1.074429000000
S	-1.907007000000	1.127296000000	0.615580000000
S	0.117519000000	1.789651000000	1.074427000000

S_8 (E)

0 1

S	0.083427000000	-1.377613000000	-1.441310000000
S	-1.860207000000	-0.705107000000	-0.265827000000
S	-1.677011000000	1.422581000000	-0.659278000000
S	-0.224162000000	2.046085000000	0.565324000000
S	-1.431758000000	-1.084638000000	1.546483000000
S	1.238110000000	-1.798388000000	0.045512000000
S	2.318113000000	-0.005769000000	0.627572000000
S	1.553488000000	1.502850000000	-0.418476000000

S_8 (F)

0 1

S	0.805300000000	2.036868000000	0.522043000000
S	-1.062932000000	1.753543000000	-0.181287000000
S	-1.635837000000	-0.191284000000	0.542604000000
S	-0.403817000000	-1.465671000000	-0.761135000000
S	-3.449150000000	-0.374439000000	-0.078629000000
S	2.020862000000	0.925031000000	-0.774426000000
S	2.668717000000	-0.623732000000	0.303114000000
S	1.056856000000	-2.060316000000	0.427717000000

$^3S_8$ (G)
0 3

S	0.247768000000	-1.653140000000	-0.068722000000
S	-0.672172000000	-0.517862000000	1.393217000000
S	-1.058894000000	1.280783000000	0.577455000000
S	-3.008548000000	1.074539000000	-0.314335000000
S	2.256813000000	-1.441768000000	0.219611000000
S	2.806848000000	0.181687000000	-0.994245000000
S	2.723201000000	1.817649000000	0.039142000000
S	-3.295016000000	-0.741888000000	-0.852124000000

S_8 (H)
0 1

S	-3.043644000000	-0.501160000000	0.387001000000
S	2.122475000000	-0.222965000000	-1.136619000000
S	0.576997000000	-1.537867000000	-0.556092000000
S	0.154314000000	-1.068054000000	1.305772000000
S	3.043652000000	0.501173000000	0.386981000000
S	-2.122504000000	0.222965000000	-1.136629000000
S	-0.576974000000	1.537828000000	-0.556149000000
S	-0.154316000000	1.068080000000	1.305736000000

A4.2 Geometries optimized using CCSD/aug-cc-pV(T+d)Z

The second line for each geometry indicates the charge and the multiplicity, respectively.

A4.2.1 S_2

$^3S_2$
0 1

S	0.000000000000	0.000000000000	0.947035893466
S	0.000000000000	0.000000000000	-0.947035893466

$^1S_2$

0 1

S	0.000000000000	0.000000000000	0.952204388824
S	0.000000000000	0.000000000000	-0.952204388824

A4.2.2 S_3

linear-S_3

0 1

S	0.000000000000	0.000000000000	0.661019358124
S	0.000000000000	-1.634212255462	-0.330509679062
S	0.000000000000	1.634212255462	-0.330509679062

cyclic-S_3

0 1

S	0.000000000000	0.000000000000	1.201248235839
S	0.000000000000	-1.040311273635	-0.600624115274
S	0.000000000000	1.040311273635	-0.600624115274

linear-$^3S_3$

0 3

S	0.000000000000	0.000000000000	0.917013413835
S	0.000000000000	-1.430719795537	-0.458506706918
S	0.000000000000	1.430719795537	-0.458506706918

A4.2.3 S_4

***cis*-S_4**

0 1

S	0.000000809641	-1.608173924880	0.909395457535
S	-0.000001264734	-1.028975709575	-0.909395457535
S	0.000001264734	1.028975709575	-0.909395457535
S	-0.000000809641	1.608173924880	0.909395457535

***trans*-S_4**

0 1

S	-2.454171921236	0.206897376849	0.000000000000
S	-0.746569216133	-0.680126810854	0.000000000000
S	0.746569216133	0.680126810854	0.000000000000
S	2.454171921236	-0.206897376849	0.000000000000

***cis*-^{3}S$_4$**

0 3

S	0.177607643663	-1.744790138849	-0.873337616128
S	-0.293593893164	-1.055499004647	0.873337616128
S	0.293593893164	1.055499004647	0.873337616128
S	-0.177607643663	1.744790138849	-0.873337616128

***trans*-^{3}S$_4$**

0 3

S	-2.420446497346	0.239037200488	0.000000000000
S	-0.754460884074	-0.766874413941	0.000000000000
S	0.754460884074	0.766874413941	0.000000000000
S	2.420446497346	-0.239037200488	0.000000000000

cyclic-S$_3$(S)

0 1

S	1.220111330391	-1.048830286496	0.171077289487
S	-0.419576242689	0.000000185212	-0.692562761961
S	1.220108758590	1.048831022052	0.171077601702
S	-2.020643846292	-0.000000926060	0.350407870772

cyclic-S_4

0 1

S	0.274545000000	0.982914000000	1.046391000000
S	-0.311375000000	1.035560000000	-0.983407000000
S	0.346991000000	-0.971926000000	-1.035069000000
S	-0.310160000000	-1.046548000000	0.972085000000

trigonal-S_4

0 1

S	0.000000000000	0.000000000000	0.000000000000
S	0.000000000000	-1.645928419675	0.950277215243
S	0.000000000000	0.000000000000	-1.900554430487
S	0.000000000000	1.645928419675	0.950277215243

trigonal-$^3S_4$

0 3

S	-0.317412000000	0.320618000000	0.000000000000
S	0.952237000000	1.765458000000	0.000000000000
S	-0.317412000000	-1.043038000000	1.452581000000
S	-0.317412000000	-1.043038000000	-1.452581000000

References

(1) Grosch, H.; Fateev, A.; Clausen, S. UV absorption cross-sections of selected sulfur-containing compounds at temperatures up to 500°C. *Journal of Quantitative Spectroscopy and Radiative Transfer* **2015**, *154*, 28–34.

(2) Sunanda, K.; Shastri, A.; Das, A. K.; Raja Sekhar, B. Electronic states of carbon disulphide in the 5.5–11.8 eV region by VUV photo absorption spectroscopy. *Journal of Quantitative Spectroscopy and Radiative Transfer* **2015**, *151*, 76–87.

(3) Rabalais, J. W.; McDonald, J. R.; Scherr, V. M.; McGlynn, S. P. Electronic spectoscopy of isoelectronic molecules. II. Linear triatomic groupings containing sixteen valence electrons. *Chemical Reviews* **1971**, *71*, 73–108.

(4) Wu, C.; Chen, F. Temperature-dependent photoabsorption cross sections of H2S in the 1600–2600 Å region. *Journal of Quantitative Spectroscopy and Radiative Transfer* **1998**, *60*, 17–23.

(5) Sander, S. P.; Abbatt, J.; Barker, J. R.; Burkholder, J. B.; Friedl, R. R.; Golden, D. M.; Huie, R. E.; Kolb, C. E.; Kurylo, M. J.; Moortgat, G. K. et al. Chemical Kinetics and Photochemical Data for Use in Atmospheric Studies, Evaluation No. 17. JPL Publication 10-6, Jet Propulsion Laboratory, Pasadena, 2011; `http://jpldataeval.jpl.nasa.gov`.

(6) Limão-Vieira, P.; Ferreira da Silva, F.; Almeida, D.; Hoshino, M.; Tanaka, H.; Mogi, D.; Tanioka, T.; Mason, N. J.; Hoffmann, S. V.; Hubin-Franskin, M.-J. et al. Electronic excitation of carbonyl sulphide (COS) by high-resolution vacuum ultraviolet photoabsorption and electron-impact spectroscopy in the energy region from 4 to 11 eV. *The Journal of Chemical Physics* **2015**, *142*, 064303.

(7) Chen, F.; Judge, D. L.; Robert Wu, C. Y.; Caldwell, J.; White, H. P.; Wagener, R. High-resolution, low-temperature photoabsorption cross sections of C2H2, PH3, AsH3,

and GeH4, with application to Saturn's atmosphere. *Journal of Geophysical Research: Planets* **1991**, *96*, 17519–17527.

(8) Manatt, S. L.; Lane, A. L. A compilation of the absorption cross-sections of SO2 from 106 to 403 nm. *Journal of Quantitative Spectroscopy and Radiative Transfer* **1993**, *50*, 267–276.

(9) Burkholder, J. B.; McKeen, S. UV absorption cross sections for SO3. *Geophysical Research Letters* **1997**, *24*, 3201–3204.

(10) Hintze, P. E.; Kjaergaard, H. G.; Vaida, V.; Burkholder, J. B. Vibrational and Electronic Spectroscopy of Sulfuric Acid Vapor. *The Journal of Physical Chemistry A* **2003**, *107*, 1112–1118.

(11) Stark, G.; Herde, H.; Lyons, J. R.; Heays, A. N.; de Oliveira, N.; Nave, G.; Lewis, B. R.; Gibson, S. T. Fourier-transform-spectroscopic photoabsorption cross sections and oscillator strengths for the S2 Bu3Xg3 system. *The Journal of Chemical Physics* **2018**, *148*, 244302.

(12) Miliordos, E.; Xantheas, S. S. On the Bonding Nature of Ozone (O3) and Its Sulfur-Substituted Analogues SO2, OS2, and S3: Correlation between Their Biradical Character and Molecular Properties. *Journal of the American Chemical Society* **2014**, *136*, 2808–2817.

(13) Farahani, S.; Frandsen, B. N.; Kjaergaard, H. G.; Lane, J. R. Simulated Electronic Absorption Spectra of Sulfur-Containing Molecules Present in Earth's Atmosphere. *The Journal of Physical Chemistry A* **2019**, *123*, 6605–6617.

(14) Barbatti, M.; Sen, K. Effects of different initial condition samplings on photodynamics and spectrum of pyrrole. *International Journal of Quantum Chemistry* **2016**, *116*, 762–771.

(15) Mai, S.; Gattuso, H.; Monari, A.; González, L. Novel Molecular-Dynamics-Based Protocols for Phase Space Sampling in Complex Systems. *Frontiers in Chemistry* **2018**, *6*, 495.

(16) Prlj, A.; Hollas, D.; Curchod, B. F. E. Deciphering the Influence of Ground-State Distributions on the Calculation of Photolysis Observables. *The Journal of Physical Chemistry A* **2023**, *127*, 7400–7409.

(17) Prlj, A.; Marsili, E.; Hutton, L.; Hollas, D.; Shchepanovska, D.; Glowacki, D. R.; Slavíček, P.; Curchod, B. F. E. Calculating Photoabsorption Cross-Sections for Atmospheric Volatile Organic Compounds. *ACS Earth and Space Chemistry* **2022**, *6*, 207–217.